American Mineralogist, Volume 91, pages 1110–1116, 2006

Carbonate reduction by Fe-S-O melts at high pressure and high temperature

SARAH C. GUNN AND ROBERT W. LUTH*

C.M. Scarfe Laboratory for Experimental Petrology, Department of Earth and Atmospheric Sciences, University of Alberta, Edmonton, Alberta T6G 2E3 Canada

ABSTRACT

Diamond may form in the Earth's mantle by recrystallization of graphite, by precipitation from a C-bearing fluid, or by reduction of carbonate. The latter mechanism could result from interaction with a reduced fluid or another phase that would accommodate the oxygen produced by the reduction. One possible such phase is a sulfide-bearing melt, given that sulfides are common inclusions in diamond. Experiments at 1300 °C, 6 and 7.5 GPa successfully reduced magnesite in the presence of a eutectic-composition Fe-S-O melt. Although graphite rather than diamond was produced by this reduction, these experiments demonstrate that this mechanism is a viable mechanism for reducing carbonate to carbon in the Earth's mantle.

Keywords: Experimental petrology, high-pressure studies, igneous petrology, crystal synthesis

INTRODUCTION

Diamonds have been synthesized since the 1950s from graphite using molten transition metals as carbon solvents in high-pressure, high-temperature experiments (Bovenkerk et al. 1959). These diamonds differ in morphology, inclusions, and other characteristics from natural diamonds (Bulanova 1995), and it is unlikely that these transition metal melts are the growth media for diamonds in the Earth's mantle. A major uncertainty surrounding the formation of natural diamond is the source of carbon: is it pre-existing graphite, reduced carbon such as CH_4, or oxidized carbon such as CO_2, or carbonate? In large part, which of these possibilities are viable depends on the oxidation state of the mantle. Oxidation state is conventionally expressed in terms of the oxygen fugacity (f_{O_2}) relative to buffer reactions such as fayalite + O_2 = magnetite + quartz (FMQ) or iron + O_2 = wüstite (IW). A reaction particularly relevant to the stability of carbonate is enstatite + magnesite = forsterite + graphite or diamond + O_2, known as EMOG or EMOD depending on the carbon polymorph (Eggler and Baker 1982). This reaction dictates whether carbonate or elemental carbon will be stable in a peridotitic mineral assemblage, which is generally accepted to constitute much of the upper mantle (e.g., Green and Falloon 1998). Recent studies of garnet + olivine + orthopyroxene equilibria of mantle-derived xenoliths of samples from both the Kaapvaal and Slave cratons document f_{O_2} values between EMOG/D and IW, with f_{O_2} generally decreasing with depth (Woodland and Koch 2003; McCammon and Kopylova 2004). If these values are representative of sub-cratonic mantle, then carbonate would not be stable in the diamond stability field, at least in peridotitic parts of the mantle. In eclogite, the other major rock type of the upper mantle, the reactions that control the stability of diamond are different than those for peridotite, so the relative stabilities of carbonate and diamond in eclogite must be evaluated independently of their stability in peridotite (Luth 1993).

Experimental efforts to synthesize diamond in ways analogous to nature can be categorized as (1) solvent-assisted recrystallization of graphite, (2) oxidation of reduced carbon-bearing fluids, or (3) reduction of oxidized carbon. The first group has been the most extensively explored, with solvents or catalysts (other than transition metal melts) such as kimberlitic melts (Arima et al. 1993), solid or liquid carbonate (Akaishi et al. 1990; Taniguchi et al. 1996; Pal'yanov et al. 1999a, 1999b, 2002a; Sato et al. 1999; Sokol et al. 2000, 2001a; Spivak and Litvin 2004; Tomlinson et al. 2004), sulfide melts (Pal'yanov et al. 2001; Sato and Katsura 2001), and both oxidized (CO_2-H_2O) and reduced (CH_4-H_2O) fluids (Yamaoka et al. 1992, 2000, 2002a, 2002b; Akaishi and Yamaoka 2000; Kumar et al. 2000, 2001; Sun et al. 2000; Akaishi et al. 2000, 2001; Sokol et al. 2001b; Okada et al. 2002; Dobrzhinetskaya et al. 2004). To the authors' knowledge, no study has reported oxidation of a reduced, carbon-bearing (e.g., CH_4-rich) fluid to produce diamond in the absence of graphite or another source of carbon. Reduction of carbonate by interaction with reduced fluids (Pal'yanov et al. 2002b; Yamaoka et al. 2002c), or with Si or SiC (Arima et al. 2002) have been reported. Yamaoka et al. (2002c) reduced $CaCO_3$ to graphite, which then recrystallized to diamond at 7.7 GPa and 1500 °C, by reaction with a CH_4-H_2O fluid. Pal'yanov et al. (2002b) reduced $MgCO_3$ in the presence of SiO_2 ($\pm Na_2CO_3$) via influx of H_2 into the capsule. Although CH_4-H_2O or even H_2 fluids might be present in the mantle at f_{O_2} > IW, the presence of either Si or SiC would require much lower oxidation states (Ulmer et al. 1998). An alternative reducing agent is sulfide melt, given the frequent occurrence of sulfide as an inclusion in diamond (Bulanova 1995). We conducted initial experiments on FeS that verified its melting temperature was too high to be molten at the experimental conditions of interest (≤1300 °C). Therefore, we explored the possibility that the eutectic liquid in the Fe-S-O system (Urakawa et al. 1987) could be a reducing agent for magnesite, the carbonate stable in the diamond stability field in

* E-mail: robert.luth@ualberta.ca

a peridotitic mineral assemblage. To simulate possible reactions in the Earth's mantle more realistically, orthopyroxene was included in the samples so that MgO liberated by the reduction of magnesite could react to form olivine via the reaction $Mg_2Si_2O_6 + 2\ MgO = 2\ Mg_2SiO_4$.

Experimental methods

The starting materials were a mixture of natural magnesite (Mt. Brussilof, British Columbia, Canada), orthopyroxene (Mg no. = 0.90) from a spinel lherzolite (KR-37, Canil et al. 1990) from Kettle River, British Columbia (Table 1), and $Fe_{70}S_{28}O_2$ (molar proportions given by subscripts). The latter was a mixture of iron powder (99.9%), FeS powder (99.9%), and Fe_2O_3 (99.945%), all from Alfa/Johnson Matthey. A series of experiments were conducted on the $Fe_{70}S_{28}O_2$ mixture (ISO-1) to confirm the melting temperature reported by Urakawa et al. (1987). These experiments ensured that the $Fe_{70}S_{28}O_2$ would be molten at the conditions of the reduction experiments. The starting composition for the carbonate reduction experiments (OMS-2) was a mixture of orthopyroxene, magnesite, and $Fe_{70}S_{28}O_2$ in 4:8:1 (molar) respective proportions. To confirm that the presence of $Fe_{70}S_{28}O_2$ is required for the reduction of magnesite, a sulfide-free experiment with just orthopyroxene and magnesite in the same proportions as in OMS-2 was run.

Samples were loaded in MgO capsules, 2.3 mm outer diameter and 4.2 mm long, with a sample volume of 1 mm diameter by 1.8 mm long. The loaded capsules were dried at 120 °C for ≥14 h before being incorporated into the sample assembly. The sample assemblies consisted of a semi-sintered MgO + 5% Cr_2O_3 octahedron of 18 mm edge length containing a stepped graphite furnace surrounded by a ZrO_2 sleeve. Inside the furnace, an MgO sleeve separates the capsule from the furnace, and MgO spacers above and below the capsule center it in the assembly. A $W_{95}Re_5$-$W_{74}Re_{26}$ thermocouple, housed in an alumina (99.98% purity) sleeve, is inserted axially through the top MgO spacer. Prior to the experiment, the assembly (without the sample capsule) is heated for an hour at 1000 °C in an N_2-2%H_2 gas flow to minimize possible adsorbed H_2O. This assembly and drying procedure is the same as that used in previous studies in this laboratory (e.g., Walter et al. 1995; Luth 1997, 2001; Knoche et al. 1999).

All experiments were run in the USSA-2000 split-sphere multiple-anvil apparatus in the C.M. Scarfe Laboratory for Experimental Petrology at the University of Alberta. The pressure calibration was based on experimental brackets at 1000 °C of the quartz-coesite transition in SiO_2 at 2.95 GPa (Bohlen 1984), the garnet-perovskite transition in $CaGeO_3$ at 6.1 GPa (Susaki et al. 1985), and the coesite-stishovite transition in SiO_2 at 9.1 GPa (Yagi and Akimoto 1976), as detailed in Walter et al. (1995). Based on the reproducibility of the calibration experiments, the uncertainty in pressure is estimated to be ~0.5 GPa.

Experiments were brought to run pressure, then heated at ~70 °C/min to run temperature, and maintained at ±5 °C. No correction for pressure was applied to the *Emf* of the thermocouple. Temperature gradients within the sample capsule are estimated to be <50 °C, based on two-pyroxene geothermometry (Walter et al. 1995). After the experiment, the run was quenched by turning off the power to the furnace, followed by decompression over ~4 h.

After the run, the MgO capsule was extracted by cutting the furnace assembly away from the capsule with a low-speed diamond saw. For the ISO-1 experiments, which were conducted to constrain the melting temperature of the $Fe_{70}S_{28}O_2$ composition, the entire capsule was embedded in an epoxy plug. The plug was then ground down to expose a longitudinal section through the capsule. To preserve the texture as much as possible, the surface was repeatedly vacuum-impregnated with epoxy during the grinding process once the capsule wall was breached. After grinding and polishing, the samples were carbon-coated and examined with a JEOL 8900R electron microprobe, using backscattered electron imaging for textural examination and EDS for qualitative phase identification.

The sample treatment for the OMS-2 carbonate-reduction experiments was more involved. Initially, we examined fragments of the charge on a JEOL 6301F field emission scanning electron microscope, but the abundant sulfide and silicate matrix made it difficult to ascertain the fate of the carbonate, so a sequential acid treatment was developed. The initial step removed the bulk of the sulfide by addition of a 1:2 (v/v) mixture of hydrochloric and nitric acids to the samples in Teflon vials and heating at ~70 °C for 30 min. We then treated the samples sequentially with hydrofluoric acid to remove silicates, nitric acid to ensure all sulfide was removed, and hydrochloric acid to remove carbonate. Resultant samples, and some intermediate samples, were examined on the SEM, which is equipped with an EDS detector capable of light element (C) detection.

To examine the textural relationships between the coexisting phases and to analyze the phases in these experiments, we conducted a second series in which the entire capsule was mounted in an epoxy plug and prepared in the same fashion as the ISO-1 experiments for examination with the electron microprobe. Quantitative analyses were obtained by WDS analysis with the JEOL 8900R microprobe. Analyses were done at 15 kV accelerating voltage and beam currents (as measured on a Faraday cup) of 15 nA for silicates and sulfides, and 7 nA for carbonates. Standards used for olivine were Fo_{93} (Mg, Si) and fayalite (Fe) olivines. For garnet, pyrope (Mg, Al, Si), almandine-grossular (Fe), and grossular (Ca). For carbonate, dolomite (Mg, Ca) and hematite (Fe). For ferroan periclase, periclase (Mg), hematite (Fe). For sulfides, Fe metal (Fe) and pyrite (S).

Table 1. Composition of natural orthopyroxene KR-37 used in experiments (wt%)

SiO_2	55.74 (0.20)
TiO_2	0.04 (0.03)
Al_2O_3	3.43 (0.19)
Cr_2O_3	0.39 (0.04)
FeO	5.92 (0.01)
MnO	0.12 (0.01)
MgO	33.91 (0.12)
CaO	0.56 (0.050
Na_2O	0.04 (0.01)
NiO	0.10 (0.01)
Total	100.24 (0.23)

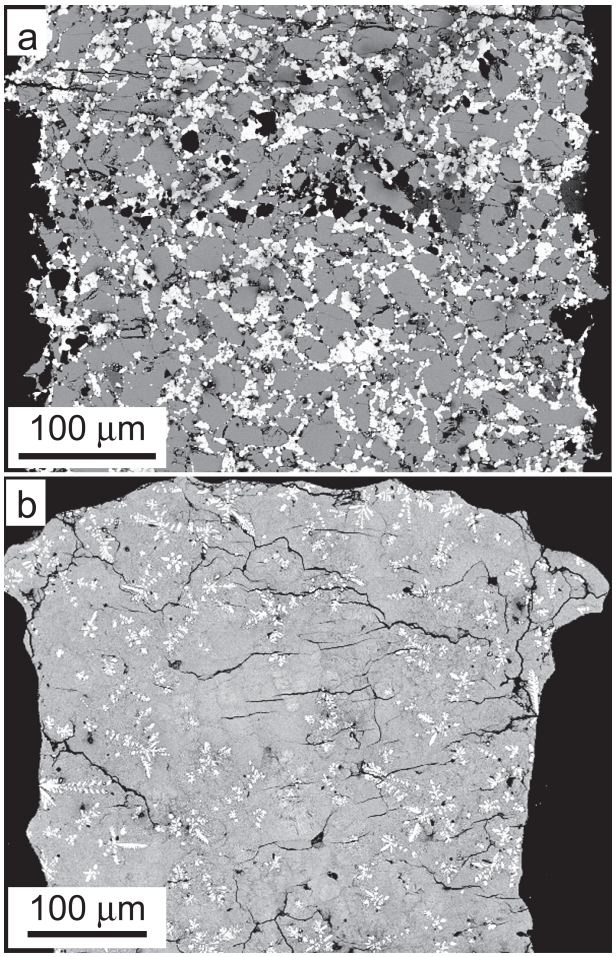

Figure 1. Backscattered electron images of phase equilibrium experiments on $Fe_{70}S_{28}O_2$ to determine melting relationships. (**a**) 6 GPa, 900 °C (no. 3504): gray is Fe_xS, white is Fe, and interstital black is Fe_xO; black regions on sides of image are the MgO capsule. (**b**) 6 GPa, 1000 °C (no. 3517): gray is Fe_xS and white is Fe. Note dendritic texture of Fe. Black regions on sides and top of image are the MgO capsule.

RESULTS

The experimental run conditions and results are given in Table 2. The run products from the ISO-1 experiments on the $Fe_{70}S_{28}O_2$ composition showed a marked change in texture between 900 and 1000 °C. At 900 °C and below, the texture was granular, with large grains of Fe_xS and minor Fe_xO, with interstitial Fe (Fig. 1a). At 1000 °C and above, the experiments contained distinctive metal dendrites in a quench mat of Fe-S-O (Fig. 1b). This melting behavior is consistent with the work of Urakawa et al. (1987), who found the eutectic at 930±10 °C at 6 GPa.

Experiment 3548, which contained orthopyroxene and magnesite but no sulfide, produced an assemblage of olivine + magnesite + garnet (Table 2). No elemental carbon was observed in this experiment. The presence of olivine, rather than orthopyroxene, may result from reaction of the starting orthopyroxene with the MgO capsule via a reaction such as $Mg_2Si_2O_6$ (opx) + 2 MgO (capsule) = 2 Mg_2SiO_4 (olivine). The survival of magnesite argues against production of olivine via the reaction $Mg_2Si_2O_6$ (opx) + 2 $MgCO_3$ (mgs) = 2 Mg_2SiO_4 + 2 C + 2 O_2, as this reaction would have consumed all the magnesite in the sample. The extremely magnesian nature of the olivine (Table 3) may be a result of incorporation of Fe into the MgO capsule as well as into the coexisting garnet (Table 4) and carbonate (Table 5).

The presence of garnet is explicable because the starting orthopyroxene contained Ca and Al, neither of which substitutes readily into olivine. Garnet would form by a reaction such as $Mg_2Si_2O_6$ (opx) + $CaAl_2SiO_6$ (opx) = $Mg_2CaAl_2Si_3O_{12}$ (grt) (and analogous reactions involving Fe^{2+}) to host the Al and some of the Ca. Partitioning of Ca between garnet and carbonate probably accounts for the more magnesian nature of the garnet in this

TABLE 2. Experimental run conditions and results

Starting composition	Run number	Pressure (GPa)	Temperature (°C)	Duration (h)	Results
$Fe_{70}S_{28}O_2$	3505	6	800	2	subsolidus
(ISO-1)	3504	6	900	2	subsolidus
	3517	6	1000	2	supersolidus
	3503	6	1100	2	supersolidus
	3497	6	1300	2	supersolidus
opx + mgs	3548	7.5	1300	24	(EMP) ol + mgs + grt
opx + mgs + $Fe_{70}S_{28}O_2$	3516	6	1300	6	(SEM) gr + silicate
(OMS-2)	3546	6	1300	6	(EMP) ol + grt + Fe-per + gr + 2 sulfides
	3523	6	1300	24	(SEM) gr + silicate
	3545	6	1300	24	(EMP) ol + grt + Fe-per + gr + 2 sulfides
	3524	7.5	1300	24	(SEM) gr + silicate
	3547	7.5	1300	24	(EMP) ol + grt + Fe-per + gr + 2 sulfides
	3525	7.5	1300	48	(EMP) ol + grt + Fe-per + gr + 2 sulfides

Note: Phase abbreviations: Fe-per = ferroan periclase, gr = graphite, grt = garnet, mgs = magnesite, ol = olivine.

TABLE 3. Average compositions of olivine in experimental run products

Run no.	3546	3545	3547	3525	3548
n	30	56	29	20	15
wt%					
SiO_2	39.18 (0.58)	40.29 (0.53)	40.34 (0.55)	39.74 (0.26)	41.61 (0.43)
FeO	13.60 (0.96)	11.05 (0.77)	11.20 (0.36)	10.79 (0.45)	2.03 (1.02)
MgO	46.92 (0.99)	49.26 (0.64)	49.34 (0.66)	48.55 (0.48)	55.56 (0.87)
Total	99.7 (0.75)	100.60 (0.70)	100.88 (0.79)	99.08 (0.48)	99.20 (0.74)
Cations per 4 O atoms					
Si	0.982 (0.009)	0.987 (0.007)	0.986 (0.010)	0.988 (0.004)	0.992 (0.004)
Fe	0.285 (0.021)	0.227 (0.017)	0.229 (0.008)	0.224 (0.010)	0.041 (0.020)
Mg	1.752 (0.030)	1.799 (0.017)	1.798 (0.017)	1.799 (0.012)	1.975 (0.024)
Total	3.019 (0.009)	3.013 (0.007)	3.014 (0.011)	3.012 (0.004)	3.008 (0.004)
Mg no.	86.0 (1.1)	88.8 (0.8)	88.7 (0.3)	88.9 (0.5)	98.0 (1.0)

Notes: n = number of analytical points in average.
Numbers in parentheses are 1 σ.

TABLE 4. Average compositions of garnet in experimental run products

Run no.	3546	3545	3547	3525	3548
n	8	14	6	8	1
wt%					
SiO_2	39.20 (0.39)	39.48 (0.25)	38.99 (0.22)	39.29 (0.27)	42.84
Al_2O_3	20.05 (0.45)	20.23 (0.38)	17.18 (1.42)	17.94 (0.92)	23.18
FeO	7.04 (0.58)	6.51 (0.64)	7.41 (0.45)	7.24 (0.89)	3.76
MgO	6.28 (0.25)	6.23 (0.58)	11.12 (4.26)	7.00 (1.31)	22.87
CaO	26.09 (0.94)	26.51 (1.26)	23.68 (2.83)	27.21 (2.32)	5.44
Total	98.66 (0.61)	98.95 (0.41)	98.39 (0.37)	98.69 (0.40)	98.10
Cations per 12 O atoms					
Si	2.995 (0.013)	3.001 (0.016)	2.989 (0.027)	3.023 (0.012)	3.029
Al	1.806 (0.032)	1.813 (0.029)	1.553 (0.134)	1.627 (0.073)	1.932
Fe	0.450 (0.036)	0.414 (0.040)	0.475 (0.029)	0.466 (0.055)	0.223
Mg	0.715 (0.027)	0.706 (0.065)	1.269 (0.482)	0.803 (0.145)	2.411
Ca	2.136 (0.087)	2.159 (0.108)	1.946 (0.238)	2.245 (0.207)	0.412
Total	8.102 (0.016)	8.093 (0.009)	8.234 (0.088)	8.164 (0.028)	8.005

Notes: Numbers in parentheses are 1 σ. Garnet grains in 3548 were very small; only one satisfactory analysis was obtained.
n = number of analytical points in average.

TABLE 5. Average composition of carbonate in run product of opx + magnesite experiment

Run no.	3548
n	6
wt%	
MgO	39.63 (0.52)
FeO	1.6 (0.49)
CaO	5.35 (1.12)
Total	46.58 (0.31)
Cation proportions	
Mg	0.893 (0.013)
Fe	0.020 (0.006)
Ca	0.087 (0.018)

Notes: n = number of analytical points in average.
Numbers in parentheses are 1 σ.

experiment relative to those found in the OMS-2 experiments (below), in which the carbonate decomposed to form graphite.

The initial three experiments (3516, 3523, and 3524) on the OMS-2 orthopyroxene + magnesite + $Fe_{70}S_{28}O_2$ composition, in which the dissolution procedure was followed, all produced hexagonal plates of carbon that we interpret to be graphite (Table 2, Fig. 2) by reduction of the magnesite. Qualitative analysis with the EDS on the SEM confirmed these crystals were carbon.

Changing the run duration from 6 h (3516) to 24 h (3523) at 6 GPa did not produce diamond rather than graphite. The experiment at 7.5 GPa tested the possibility that overstepping the graphite = diamond reaction by another 1.5 GPa would suffice to crystallize diamond rather than graphite during the experiment, but graphite precipitated in that experiment as well.

The second series of experiments on OMS-2 (3546, 3545, and 3547) were conducted to elucidate the textural relationships between the coexisting phases, and their compositions. All three of these had identical textures (Fig. 3), with clusters of olivine ± garnet ± ferroan periclase in a matte consisting of blebs of FeS with intersitial sulfide of ~Fe_2S composition (Table 6, Table 7). This interstitial sulfide displayed submicrometer dendritic textures (Fig. 4), suggestive of quench crystallization. It is unclear, however, if the blebs of FeS are also a product of quench crystallization or represent stable solid sulfide at the conditions of the experiments.

The olivine in these experiments are magnesian (Fo_{86}-Fo_{89}), but less so than that produced in the opx + mgs experiment described above. Similarly, the garnet compositions are more calcic than that in the opx + mgs experiment (Table 4). These differences are probably the result of the absence of magnesite as a significant sink for Fe and Ca, as well as the presence of sulfide (Table 6) and ferroan periclase (Table 7) that will influence the silicate compositions by partitioning of Fe and, in the case of ferroan periclase, Mg as well.

Also present in these experiments are narrow crystals of carbon (Fig. 3); we interpret their morphology to represent cross-sections (at varying orientations) through the type of platy crystals observed in the initial experiments (Fig. 2). As noted previously, we interpret these crystals to be graphite based on their morphology and composition.

Qualitative analysis with the EDS on the SEM confirmed that the rod-like crystal sections observed in the polished probe sections (Fig. 3) are carbon. An EDS spectrum of one of the crystals from Experiment 3525 is shown in Figure 5, with a spectrum of the interstitial Fe_2S material for comparison. The

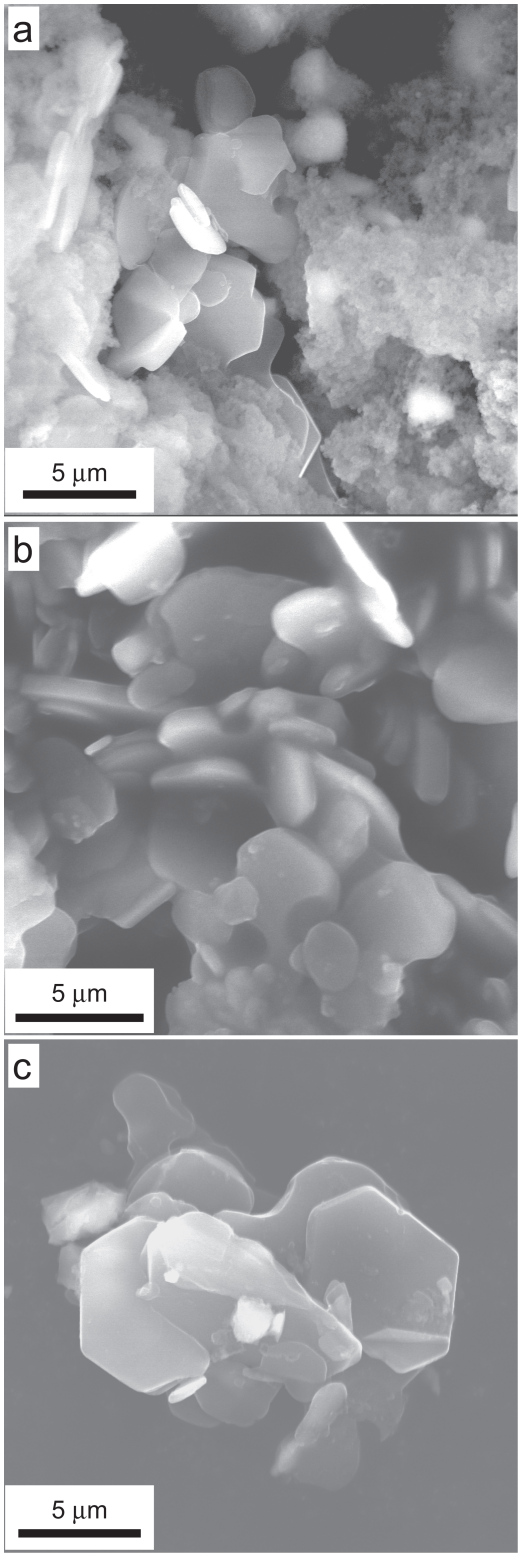

FIGURE 2. (**a**) SEM image of hexagonal plates of graphite intergrown with silicates from 6 GPa, 1300 °C, 6 h experiment (no. 3516). Sample treated with HCl-HNO_3 only. (**b**) SEM image of plates of graphite from the same experiment after sequential acid treatment. (**c**) SEM image of plates of graphite from 6 GPa, 1300 °C, 24 h experiment (no. 3523) after sequential acid treatment.

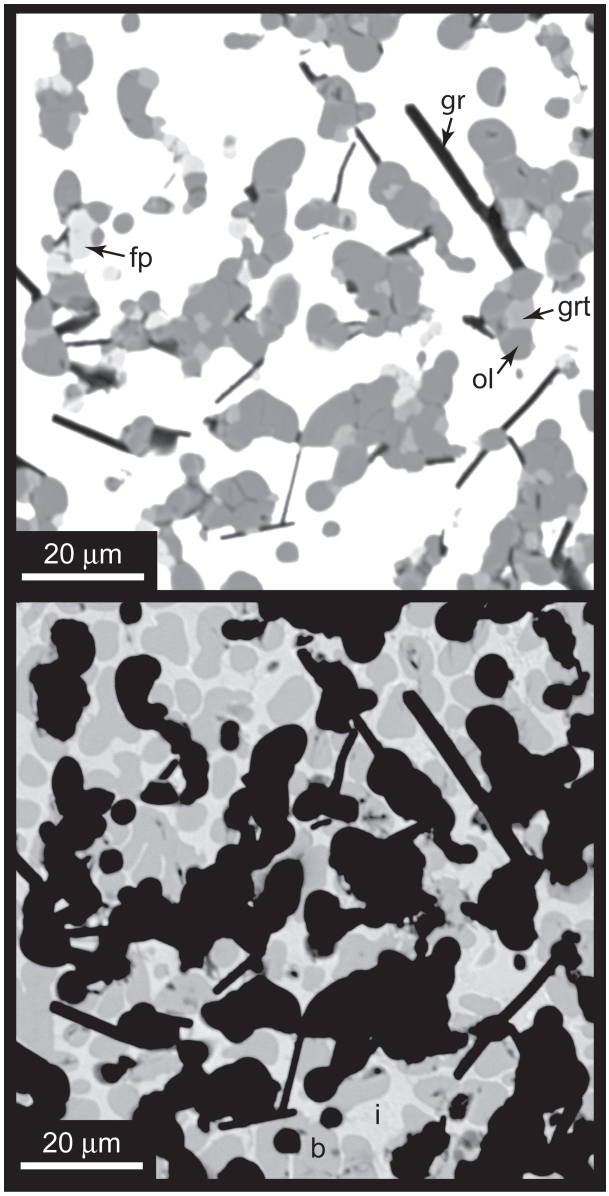

FIGURE 3. Backscattered electron image of textures and phases present in Experiment 3525. Identical textures were observed in other OMS-2 experiments that were imaged with the electron microprobe and SEM. Because of the wide range of mean atomic weights of the phases, the same area is shown in the top and bottom images with different grayscales to resolve the silicates and carbon (top) and the sulfides (bottom). The top image shows the textural relationships of the olivine (ol), garnet (grt), ferroan periclase (fp), and graphite (gr). Note the thin nature of the graphite "rods," which are interpreted to be cross-sections of sheet-like crystals as seen in Figure 2. The bottom image illustrates the relationship between the "blebs" of FeS (b) and the interstitial (i) material of ~Fe_2S composition.

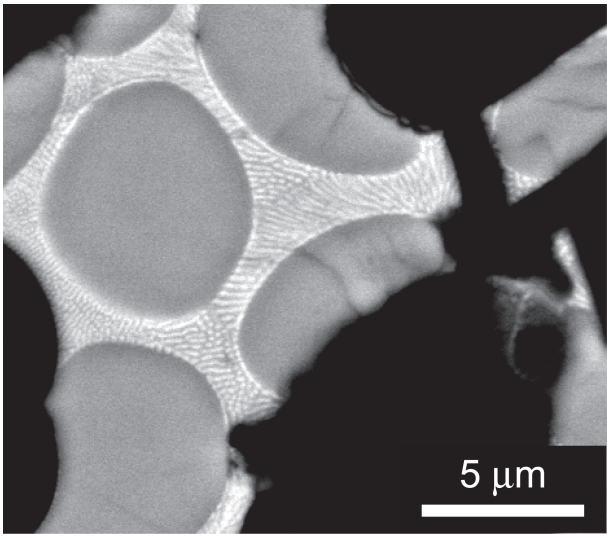

FIGURE 4. Backscattered electron image of Experiment 3525, showing submicrometer dendritic intergrowth in interstitial sulfide. See text for discussion.

TABLE 6. Average compositions of sulfides in experimental run products

Run no.	3546 blebs	3546 interstitial	3545 blebs	3545 interstitial
n	9	10	22	18
wt%				
Fe	63.38 (0.53)	77.68 (0.41)	63.43 (0.37)	76.82 (1.08)
S	35.94 (0.31)	21.33 (0.35)	36.06 (0.31)	21.98 (0.84)
Total	99.32 (0.36)	99.01 (0.36)	99.49 (0.25)	98.80 (0.37)
Atomic proportions				
Fe	50.306 (0.398)	67.646 (0.433)	50.243 (0.338)	66.742 (1.148)
S	49.694 (0.398)	32.354 (0.433)	49.757 (0.338)	33.258 (1.148)

TABLE 6. *Continued*

Run no.	3547 blebs	3547 interstitial	3525 blebs	3525 interstitial
n	21	16	14	12
wt%				
Fe	63.27 (0.25)	77.81 (1.44)	63.71 (0.45)	78.8 (0.70)
S	35.95 (0.26)	21.07 (1.31)	36.20 (0.42)	20.55 (0.63)
Total	99.21 (0.19)	98.88 (0.30)	99.91 (0.44)	99.35 (0.32)
Atomic proportions				
Fe	50.255 (0.264)	67.965 (1.723)	50.259 (0.410)	68.759 (0.835)
S	49.745 (0.264)	32.036 (1.723)	49.741 (0.410)	31.241 (0.835)

Notes for both parts of Table 6: n = number of analytical points in average. Numbers in parentheses are 1 σ.

TABLE 7. Average compositions of ferroan periclase in experimental run products

Run no.	3546	3545	3547	3525
n	15	13	17	7
wt%				
MgO	45.47 (0.35)	49.32 (1.28)	45.59 (0.63)	49.35 (1.11)
FeO	53.80 (0.47)	50.03 (1.43)	54.33 (0.90)	51.67 (0.97)
Total	99.26 (0.46)	99.35 (0.66)	99.92 (0.68)	101.02 (0.43)
Cation proportions:				
Mg	0.601 (0.003)	0.637 (0.012)	0.599 (0.007)	0.63 (0.009)
Fe	0.399 (0.003)	0.363 (0.012)	0.401 (0.007)	0.37 (0.009)

Notes: n = number of analytical points in average. Numbers in parentheses are 1σ.

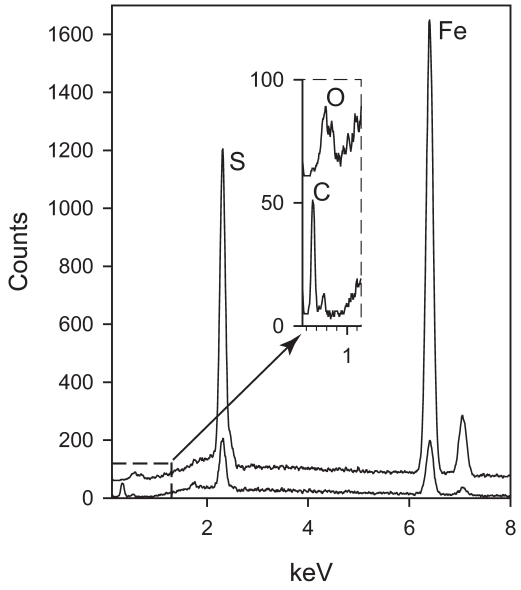

FIGURE 5. Energy-dispersive spectrum of interstitial Fe_2S phase (top spectrum, offset by 60 counts vertically to avoid overlap) and graphite (bottom spectrum) from Experiment 3525. The diameter of the activation volume of the beam is wider than the cross-section of the graphite crystal, so there are contributions in this spectrum from the surrounding sulfide and silicate material. Inset shows low-energy region at expanded scale, showing the C peak in the graphite and the O peak in the sulfide.

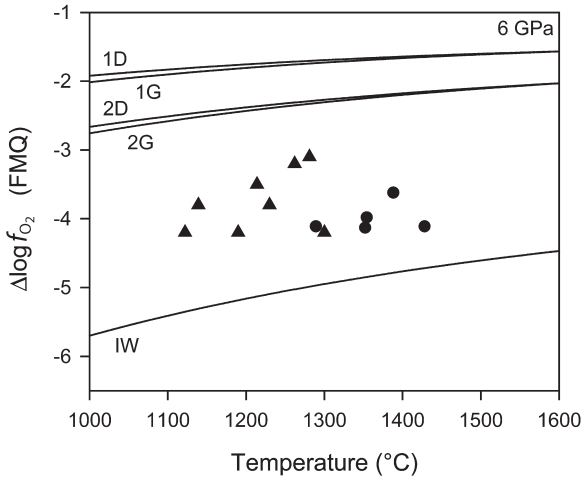

FIGURE 6. Location of possible reduction reactions in T-f_{O_2} space calculated with THERMOCALC 3.23 (Holland and Powell 1998) at 6 GPa. Oxygen fugacity expressed in log units relative to the calculated log(f_{O_2}) of the fayalite-magnetite-quartz reaction. Reactions: 1 – $Mg_2Si_2O_6$ + 2 $MgCO_3$ = 2 Mg_2SiO_4 + 2 C + 2 O_2 (Eggler and Baker 1982); 2 – $MgCO_3$ = MgO + C + O_2. In both cases, "D" and "G" refer to diamond and graphite polymorphs, respectively. For reference, the location of the IW reaction (2x Fe + O_2 = 2 Fe_xO) is plotted, using the equation from Ballhaus et al. (1991). For comparison, calculated oxygen fugacities from garnet-bearing peridotites from southern Africa (circles, Woodland and Koch 2003) and from northern Canada (triangles, McCammon and Kopylova 2004) are shown for samples with calculated pressures of 5.9–6.4 GPa.

presence of Fe, S, and Si peaks in the former spectrum is a result of the small cross-section of the crystal (~1 μm) relative to the predicted diameter of the activation volume (~3 μm at the 20 kV accelerating voltage used). The additional peaks therefore represent contributions from surrounding sulfide and silicate phases. A noteworthy feature of the Fe_2S spectrum is the presence of an oxygen peak (inset, Fig. 5), confirming that O did dissolve in the sulfide melt.

DISCUSSION

The results of this study demonstrate that a Fe-S-O melt is capable of reducing carbonate to elemental carbon, and hence is capable of dissolving sufficient oxygen to allow this process to occur, via reactions such as:

2 $MgCO_3$ (Mgs) + $Mg_2Si_2O_6$ (Opx) = 2 Mg_2SiO_4 (Ol) + 2 C (Gr) + 2 O_2 (in Fe-S-O melt), or

2 $MgCO_3$ (Mgs) = MgO (ferroan periclase) + C (Gr) + 2 O_2 (in Fe-S-O melt)

at temperatures appropriate for the mantle. The former reaction is more relevant to the mantle, but the latter reaction may have contributed in the experiments because the MgO capsule may have imposed a silica activity via the reaction Mg_2SiO_4 = 2 MgO + SiO_2 at which orthopyroxene would not be stable. Both of these possible reduction reactions occur at more oxidizing conditions than those calculated from garnet-olivine-orthopyroxene equilibria in mantle-derived xenoliths from diamondiferous mantle beneath southern Africa and northern Canada (Fig. 6). Neither of these reactions require oxidation states lower than those observed in these two studies, unlike those required by the presence of Si or SiC.

Although the run conditions were in the diamond stability field (Kennedy and Kennedy 1976; Bundy et al. 1996), the experiments produced graphite rather than diamond. This result was independent of differing run times (6–24 h at 6 GPa and 1300 °C), and of increasing pressure from 6 to 7.5 GPa to overstep the graphite-diamond reaction further. The occurrence of metastable graphite instead of diamond has been observed in previous studies at higher temperatures. For example, in the reduction of carbonate by moissanite at 7.7 GPa (Arima et al. 2002), abundant graphite formed in short duration runs; 8 h at 1600 °C and 24 h at 1500 °C was needed to nucleate diamond in that system. In their study of reduction of $CaCO_3$ by CH_4-H_2O fluid, (Yamaoka et al. 2002c) observed graphite formation within 1 h at 7.7 GPa and 1500 °C, with the graphite transforming to diamond after 12 h. Although such recrystallization may occur in longer-duration experiments in the present system, we note that 48 h at 7.5 GPa and 1300 °C was insufficient for such recrystallization to occur (Table 2, Experiment 3525). On the basis of the production of graphite, however, we still conclude that sulfide-rich melts are a potential reducing agent for carbonate in the Earth's mantle.

ACKNOWLEDGMENTS

This manuscript is based on the first author's B.Sc. Honors thesis. This research was supported by an NSERC USRA to SCG and an NSERC Discovery Grant to R.W.L. We thank Diane Caird for assistance in the high-pressure laboratory, George Braybrook and Sergei Matveev for help with the SEM and electron microprobe,

respectively, and David Selby for advice and help on dissolution of sulfides. Constructive reviews of an earlier version of this manuscript by two anonymous reviewers and comments by Associate Editor Alison Pawley were of great use in improving this manuscript.

REFERENCES CITED

Akaishi, M. and Yamaoka, S. (2000) Crystallization of diamond from C-O-H fluids under high-pressure and high-temperature conditions. Journal of Crystal Growth, 209, 999–1003.

Akaishi, M., Kanda, H., and Yamaoka, S. (1990) Synthesis of Diamond from Graphite Carbonate Systems under Very High-Temperature and Pressure. Journal of Crystal Growth, 104, 578–581.

Akaishi, M., Kumar, M.D.S., Kanda, H., and Yamaoka, S. (2000) Formation process of diamond from supercritical H_2O-CO_2 fluid under high-pressure and high-temperature conditions. Diamond and Related Materials, 9, 1945–1950.

——— (2001) Reactions between carbon and a reduced C-O-H fluid under diamond-stable HP-HT condition. Diamond and Related Materials, 10, 2125–2130.

Arima, M., Nakayama, K., Akaishi, M., Yamaoka, S., and Kanda, H. (1993) Crystallization of diamond from a silicate melt of kimberlite composition in high-pressure and high-temperature experiments. Geology, 21, 968–970.

Arima, M., Kozai, Y., and Akaishi, M. (2002) Diamond nucleation and growth by reduction of carbonate melts under high-pressure and high-temperature conditions. Geology, 30, 691–694.

Ballhaus, C., Berry, R.F., and Green, D.H. (1991) High-pressure experimental calibration of the olivine-orthopyroxene-spinel oxygen geobarometeróImplications for the oxidation state of the upper mantle. Contributions to Mineralogy and Petrology, 107, 27–40.

Bohlen, S.R. (1984) Equilibria for precise pressure calibration and a frictionless furnace assembly for the piston-cylinder apparatus. Neues Jahrbuch Fur Mineralogie-Monatshefte, 404–412.

Bovenkerk, H.P., Bundy, F.P., Hall, H.T., Strong, H.M., and Wentorf, R.H. (1959) Preparation of diamond. Nature, 184, 1094–1098.

Bulanova, G.P. (1995) The Formation of diamond. Journal of Geochemical Exploration, 53, 1–23.

Bundy, F.P., Bassett, W.A., Weathers, M.S., Hemley, R.J., Mao, H.K., and Goncharov, A.F. (1996) The pressure-temperature phase and transformation diagram for carbon; Updated through 1994. Carbon, 34, 141–153.

Canil, D., Virgo, D., and Scarfe, C.M. (1990) Oxidation state of mantle xenoliths from British Columbia, Canada. Contributions to Mineralogy and Petrology, 104, 453–462.

Dobrzhinetskaya, L.F., Renfro, A.P., and Green, H.W. (2004) Synthesis of skeletal diamonds: Implications for microdiamond formation in orogenic belts. Geology, 32, 869–872.

Eggler, D.H. and Baker, D.R. (1982) Reduced volatiles in the system C-O-H: Implications to mantle melting, fluid formation, and diamond genesis. In S. Akimoto and M.H. Manghnani, Eds., High-pressure research in geophysics, 12, p. 237–250. Center for Academic Publications, Tokyo.

Green, D.H. and Falloon, T.J. (1998) Pyrolite: A Ringwood concept and its current expression. In I. Jackson, Ed., The Earth's Mantle: Composition, Structure, and Evolution, p. 311–378. Cambridge University Press, Cambridge.

Holland, T.J.B. and Powell, R. (1998) An internally consistent thermodynamic data set for phases of petrological interest. Journal of Metamorphic Geology, 16, 309–343.

Kennedy, C.S. and Kennedy, G.C. (1976) Equilibrium boundary between graphite and diamond. Journal of Geophysical Research, 81, 2467–2470.

Knoche, R., Sweeney, R.J., and Luth, R.W. (1999) Carbonation and decarbonation of eclogites: the role of garnet. Contributions to Mineralogy and Petrology, 135, 332–339.

Kumar, M.D.S., Akaishi, M., and Yamaoka, S. (2000) Formation of diamond from supercritical H_2O-CO_2 fluid at high pressure and high temperature. Journal of Crystal Growth, 213, 203–206.

——— (2001) Effect of fluid concentration on the formation of diamond in the CO_2-H_2O-graphite system under HP-HT conditions. Journal of Crystal Growth, 222, 9–13.

Luth, R.W. (1993) Diamonds, eclogites, and the oxidation state of the Earth's mantle. Science, 261, 66–68.

——— (1997) Experimental study of the system phlogopite-diopside from 3.5 to 17 GPa. American Mineralogist, 82, 1198–1209.

——— (2001) Experimental determination of the reaction aragonite plus magnesite = dolomite at 5 to 9 GPa. Contributions to Mineralogy and Petrology, 141, 222–232.

McCammon, C. and Kopylova, M.G. (2004) A redox profile of the Slave mantle and oxygen fugacity control in the cratonic mantle. Contributions to Mineralogy and Petrology, 148, 55–68.

Okada, T., Utsumi, W., Kaneko, H., Yamakata, M., and Shimomura, O. (2002) In situ X-ray observations of the decomposition of brucite and the graphite-diamond conversion in aqueous fluid at high pressure and temperature. Physics and Chemistry of Minerals, 29, 439–445.

Pal'yanov, Y., Borzdov, Y., Kupriyanov, I., Gusev, V., Khokhryakov, A., and Sokol, A. (2001) High-pressure synthesis and characterization of diamond from a sulfur-carbon system. Diamond and Related Materials, 10, 2145–2152.

Pal'yanov, Y.N., Sokol, A.G., Borzdov, Y.M., Khokhryakov, A.F., Shatsky, A.F., and Sobolev, N.V. (1999a) The diamond growth from Li_2CO_3, Na_2CO_3, K_2CO_3, and Cs_2CO_3 solvent-catalysts at P = 7 GPa and T = 1700–1750 degrees C. Diamond and Related Materials, 8, 1118–1124.

Pal'yanov, Y.N., Sokol, A.G., Borzdov, Y.M., Khokhryakov, A.F., and Sobolev, N.V. (1999b) Diamond formation from mantle carbonate fluids. Nature, 400, 417–418.

Pal'yanov, Y.N., Sokol, A.G., Borzdov, Y.M., and Khokhryakov, A.F. (2002a) Fluid-bearing alkaline carbonate melts as the medium for the formation of diamonds in the Earth's mantle: an experimental study. Lithos, 60, 145–159.

Pal'yanov, Y.N., Sokol, A.G., Borzdov, Y.M., Khokhryakov, A.F., and Sobolev, N.V. (2002b) Diamond formation through carbonate-silicate interaction. American Mineralogist, 87, 1009–1013.

Sato, K. and Katsura, T. (2001) Sulfur: a new solvent-catalyst for diamond synthesis under high-pressure and high-temperature conditions. Journal of Crystal Growth, 223, 189–194.

Sato, K., Akaishi, M., and Yamaoka, S. (1999) Spontaneous nucleation of diamond in the system $MgCO_3$-$CaCO_3$-C at 7.7 GPa. Diamond and Related Materials, 8, 1900–1905.

Sokol, A.G., Tomilenko, A.A., Pal'yanov, Y.N., Borzdov, Y.M., Pal'yanova, G.A., and Khokhryakov, A.F. (2000) Fluid regime of diamond crystallisation in carbonate-carbon systems. European Journal of Mineralogy, 12, 367–375.

Sokol, A.G., Borzdov, Y.M., Pal'yanov, Y.N., Khokhryakov, A.F., and Sobolev, N.V. (2001a) An experimental demonstration of diamond formation in the dolomite-carbon and dolomite-fluid-carbon systems. European Journal of Mineralogy, 13, 893–900.

Sokol, A.G., Pal'yanov, Y.N., Pal'yanova, G.A., Khokhryakov, A.F., and Borzdov, Y.M. (2001b) Diamond and graphite crystallization from C-O-H fluids under high-pressure and high-temperature conditions. Diamond and Related Materials, 10, 2131–2136.

Spivak, A.V. and Litvin, Y.A. (2004) Diamond syntheses in multicomponent carbonate-carbon melts of natural chemistry: elementary processes and properties. Diamond and Related Materials, 13, 482–487.

Sun, L.L., Akaishi, M., and Yamaoka, S. (2000) Formation of diamond in the system of Ag_2CO_3 and graphite at high pressure and high temperatures. Journal of Crystal Growth, 213, 411–414.

Susaki, J., Akaogi, M., Akimoto, S., and Shimomura, O. (1985) Garnet-perovskite transformation in $CaGeO_3$—Insitu X-Ray measurements using synchrotron radiation. Geophysical Research Letters, 12, 729–732.

Taniguchi, T., Dobson, D., Jones, A.P., Rabe, R., and Milledge, H.J. (1996) Synthesis of cubic diamond in the graphite-magnesium carbonate and graphite-$K_2Mg(CO_3)_2$ systems at high pressure of 9–10 GPa region. Journal of Materials Research, 11, 2622–2632.

Tomlinson, E., Jones, A., and Milledge, J. (2004) High-pressure experimental growth of diamond using C-K_2CO_3-KCl as an analogue for Cl-bearing carbonate fluid. Lithos, 77, 287–294.

Ulmer, G.C., Grandstaff, D.E., Woermann, E., Gobbels, M., Schonitz, M., and Woodland, A.B. (1998) The redox stability of moissanite (SiC) compared with metal-metal oxide buffers at 1773 K and at pressures up to 90 kbar. Neues Jahrbuch Fur Mineralogie-Abhandlungen, 172, 279–307.

Urakawa, S., Kato, M., and Kumazawa, M. (1987) Experimental study on the phase relations in the system Fe-Ni-O-S to 15 GPa. In M.H. Manghnani and Y. Syono, Eds., High-pressure research in mineral physics, 39, p. 95–111. American Geophysical Union, Washington, D.C.

Walter, M.J., Thibault, Y., Wei, K., and Luth, R.W. (1995) Characterizing experimental pressure and temperature conditions in multi-anvil apparatus. Canadian Journal of Physics, 73, 273–286.

Woodland, A.B. and Koch, M. (2003) Variation in oxygen fugacity with depth in the upper mantle beneath the Kaapvaal craton, Southern Africa. Earth and Planetary Science Letters, 214, 295–310.

Yagi, T. and Akimoto, S.I. (1976) Direct determination of coesite-stishovite transition by in situ X-Ray measurements. Tectonophysics, 35, 259–270.

Yamaoka, S., Akaishi, M., Kanda, H., and Osawa, T. (1992) Crystal growth of diamond in the system of carbon and water under very high pressure and temperature. Journal of Crystal Growth, 125, 375–377.

Yamaoka, S., Kumar, S., Akaishi, M., and Kanda, H. (2000) Reaction between carbon and water under diamond-stable high-pressure and high-temperature conditions. Diamond and Related Materials, 9, 1480–1486.

Yamaoka, S., Kumar, M.D.S., Kanda, H., and Akaishi, M. (2002a) Crystallization of diamond from CO_2 fluid at high pressure and high temperature. Journal of Crystal Growth, 234, 5–8.

——— (2002b) Thermal decomposition of glucose and diamond formation under diamond-stable high pressure-high temperature conditions. Diamond and Related Materials, 11, 118–124.

——— (2002c) Formation of diamond from $CaCO_3$ in a reduced C-O-H fluid at HP-HT. Diamond and Related Materials, 11, 1496–1504.

MANUSCRIPT RECEIVED JUNE 15, 2005
MANUSCRIPT ACCEPTED FEBRUARY 11, 2006
MANUSCRIPT HANDLED BY ALISON PAWLEY